

Unusual Conformational Behavior of Complexes of Poly(*N*-isopropylacrylamide) with Poly(methacrylic acid)

Tatiana V. Burova,^{*,†} Natalia V. Grinberg,[†] Valerij Ya. Grinberg,[†] Elena V. Kalinina,[‡] Vladimir I. Lozinsky,[‡] Vladimir O. Aseyev,[§] Susanna Holappa,[§] Heikki Tenhu,[§] and Alexei R. Khokhlov[‡]

N.M. Emanuel Institute of Biochemical Physics, Russian Academy of Sciences, Vavilov St. 28, 119991, Moscow, Russia; A.N. Nesmeyanov Institute of Organoelement Compounds, Russian Academy of Sciences, Vavilov St. 28, 119991 Moscow, Russia; and University of Helsinki, PB 55, FIN-00014 Helsinki, Finland

Received June 30, 2004; Revised Manuscript Received November 17, 2004

ABSTRACT: Hydrogen-bonded interpolymer complexes between poly(*N*-isopropylacrylamide) (pNIPA) and poly(methacrylic acid) (pMAA) were studied in aqueous solutions by means of high-sensitivity differential scanning calorimetry (HS-DSC), analytical ultracentrifugation, and light scattering. Composition of the complexes was varied by changing the pMAA/pNIPA molar ratio r and pH. Solubility of the pMAA/pNIPA complexes increased with increasing the content of pMAA in the complex and decreased with decreasing pH. According to HS-DSC, the phase transition behavior of pNIPA upon heating is significantly modified in complexes with pMAA. Thus, decreasing pH from pH 7 to 3 or increasing the content of pMAA decreases the phase transition temperature of the complexes by 4–5 °C with respect to the lower critical solution temperature (LCST) of pure pNIPA. At the same time, the enthalpy of the transition decreases down to zero and the transition width increases by more than 1 order of magnitude. Thermograms of the soluble complexes ($4.3 < \text{pH} < 6.3$, $r = 2.7$) show an additional cooperative transition preceding the phase separation upon heating. This transition is accompanied by increasing the sedimentation coefficient of the complexes and decreasing their mean hydrodynamic diameter. Experimental data suggest that the pMAA/pNIPA complexes are able to fold cooperatively to a compact structure without a loss of solubility at temperatures below the LCST of pNIPA.

Introduction

Design of polymer systems (chains, networks, and nanoparticles) displaying typical protein-like properties became a problem of increasing interest from both fundamental and biotechnological points of view.^{1,2} Generally, the protein-like behavior implies a cooperative response of macromolecules to the changing environment (temperature, pH, ionic strength, etc.) without a change in the macrophase state of the system, i.e., without precipitation in a wide range of polymer concentrations. The unique primary structure of proteins makes such behavior possible. Thermosensitive linear polymers with lower critical solution temperature (LCST), such as poly(*N*-isopropylacrylamide) (pNIPA)^{3–9} or poly(*N*-vinylcaprolactam) (pNVCL),^{10–12} have been used as primary units in chemical design of “smart” macromolecules.¹³ Hydrophilization of these polymers either by bound surfactant^{12,14} or by copolymerization with hydrophilic monomers under special conditions^{10,15,16} resulted in preparation of macromolecules with protein-like properties.

Interpolymer noncovalent conjugation provides a promising possibility of adjusting the hydrophobic–hydrophilic balance in the thermosensitive polymeric systems. Intermolecular hydrogen bonding was reported for systems, involving pNIPA as a hydrophobic compo-

nent and poly(carboxylic acids) as hydrophilic ones.^{17–21} These polymers form stable interpolymer complexes in aqueous media due to the hydrogen bonds between the amide groups of pNIPA and the carboxylic groups of poly(acrylic acid) (pAA) or poly(methacrylic acid) (pMAA). Potentiometric studies showed that compositions of the complexes correspond to the equimolar ratios of the interacting groups of the polymers.^{17,18,20} Viscometric and fluorescence methods revealed a contribution of hydrophobic interactions to the stabilization of the pAA/pNIPA complexes.^{17,20} Much less is known about the interaction of pNIPA with pMAA.^{18,21} From the structural point of view, the interpolymer complexes resemble graft copolymers,^{22,23} and therefore the main features of the phase and conformational behavior can be common for the complexes and graft copolymers.^{5,9,13,22–26}

In this work we report the results of the study of the pMAA/pNIPA interpolymer complexes performed using high-sensitivity differential scanning calorimetry (HS-DSC), ultracentrifugation, and light scattering. We show that under certain conditions (pH and pMAA/pNIPA ratio) the interpolymer complexes in aqueous solutions undergo a reversible cooperative conformational transition that is not related to phase separation.

Experimental Section

Polymer Synthesis. *N*-Isopropylacrylamide (NIPA) purchased from Polyscience was used without additional purification. Ammonium persulfate (APS) was from Serva, and *N,N,N',N'*-tetramethylethylenediamine (TMEDA) was from Reanal (Hungary). TMEDA was refined by distillation in a vacuum (29–32 °C/10 mmHg). All aqueous solutions were prepared using deionized water.

[†] N.M. Emanuel Institute of Biochemical Physics, Russian Academy of Sciences.

[‡] A.N. Nesmeyanov Institute of Organoelement Compounds, Russian Academy of Sciences.

[§] University of Helsinki.

* Corresponding author: fax 7(095) 135 50 85; e-mail burova@ineos.ac.ru.

The initial aqueous solution of NIPA with concentration of 3 or 6 g dL⁻¹ was degassed in a vacuum (12 mmHg) for 15 min; afterward, the redox initiation mixture (0.02 mL of TMEDA and 0.007 g of APS per 1 g of the NIPA monomer) was added. The reaction mixture was incubated at 60 °C for 3 h, then cooled to room temperature, and dialyzed for 72 h against 100-fold excess of deionized water. The cutoff limit of the membrane used was 30 kDa. After the dialysis the polymer was isolated by freeze-drying and then dried to a constant weight in a vacuum desiccator over CaCl₂ granules. According to ultracentrifugation, the molecular weight of pNIPA was 330 kDa.

Poly(methacrylic acid) (pMAA) was polymerized using a reversible addition fragmentation transfer (RAFT) method. Initially *tert*-butyl methacrylate was polymerized, and subsequently the polymers were hydrolyzed to obtain pMAA.

4,4'-Azobis(4-cyanopentanoic acid) (ACPA) from Fluka was dried under reduced pressure at room-temperature overnight and used as initiator. The RAFT agent, 4-cyano-4-dithiobenzoylpentanoic acid, was prepared as described earlier.²⁷ Monomer *tert*-butyl methacrylate (tBMA) from Aldrich was distilled under reduced pressure. Dioxane was dried with molecular sieves and distilled under reduced pressure. Methanol, acetonitrile, chloroform, and sodium iodide from Merck and trimethylsilyl chloride (TMSCl) from Fluka were used as received.

The RAFT agent and ACPA were added to a 50 vol % mixture of tBMA and dioxane. The mixture was degassed by three freeze-thaw cycles. Subsequently, the mixture was heated to 73 °C. The polymerization was allowed to proceed for 46 h under reduced pressure and in the absence of oxygen under stirring. Poly-tBMA was isolated and purified by double precipitation in methanol/water mixture (4:1). The hydrolysis of poly-tBMA was carried out in an acetonitrile/chloroform mixture (2:1), polymer concentration 5 wt %, under nitrogen.²⁸ TMSCl and sodium iodide were added in that order into the polymer solution, and the mixture was stirred at room temperature overnight. Subsequently, the solvent was removed by evaporation. The dry residue was dissolved in water, and the polymer was purified by dialysis. The polymer was characterized by H NMR and potentiometric titration. According to the size exclusion chromatography, the molecular weight of pMAA was 24.5 kDa.

Preparation of Interpolymer Complexes. Stock solutions of pNIPA and pMAA in a buffer of choice were used for preparation of the interpolymer complexes. They were prepared by a dropwise addition of the pMAA stock solution to the pNIPA stock solution under continuous stirring. The mixtures were incubated at room temperature for about 20 h prior to the experiments. Polymer composition in the complexes was characterized by the polymer molar ratio *r*, i.e., the ratio of molar concentrations of pMAA and pNIPA macromolecules. The *r* values were calculated using the average molar weights of pNIPA and pMAA of 330 and 24.5 kDa, respectively. Interpolymer composition was varied by changing the pMAA concentration while concentration of pNIPA was kept constant (1 mg mL⁻¹). The pH of the mixtures was varied by using appropriate buffers: 10 mM sodium phosphate at pH 7.0–5.8, 10 mM sodium acetate at pH 5.7–4.0, and 10 mM glycine at pH 3.1.

High-Sensitivity Differential Scanning Calorimetry. Calorimetric measurements were carried out with the differential adiabatic scanning microcalorimeters DASM-4 (NPO Biopribor, Pushchino, Russia) and VP-DSC (MicroCal Inc.) within the temperature range 10–80 °C and under an excess pressure of 2 bar. The heating rate in most experiments was 1 °C min⁻¹. Primary data processing was performed using either the software WSCAL (Institute of Protein Research, Russia) or Origin-DSC v.4.1 (MicroCal Inc.). Transformation of the thermograms into the excess heat capacity functions was carried out using the NAIRTA software (Institute of Biochemical Physics, Moscow). A third-order polynomial was applied in most cases to approximate the transition baseline when calculating the excess heat capacity. The peak temperature of the excess heat capacity function was assumed to be the transition temperature (*T*_t). The transition enthalpy ($\Delta_t h$)

was determined by integration of the excess heat capacity function. The transition width ($\Delta_t T$) was calculated as the full width at half-maximum (fwhm) of the peak in the excess heat capacity function.

Light Scattering. Light scattering of the polymer solutions was measured with a Brookhaven Instrument BIC-200 SM goniometer and a BIC-9000 AT digital correlator. An argon laser (LEXEL 85, 1 W) attenuated for 15–50 mW output power and wavelength $\lambda = 514.5$ nm was the light source. The autocorrelation function of scattered light intensity ($G_2(t)$) was collected in the self-beating mode²⁹ and then converted into an autocorrelation function of scattered electric field ($g_1(t)$). The measurements were mostly performed at 90° scattering angle. Distributions of hydrodynamic sizes were also studied at 30° and 150° for selected solutions to ensure that the size distributions were unimodal and that relaxation times of correlation functions represented a diffusive process. Distributions of hydrodynamic radii were obtained using an inverse Laplace transform algorithm (CONTIN). The mean peak value of the size distribution was used to describe the size of the scattering particles in solution. An alternative single stretched exponent analysis of the correlation functions was applied to estimate the size distribution widths.

$$g_1(t) = A \exp\left(-\left(\frac{t}{\tau}\right)^\beta\right)$$

The autocorrelation function of the scattered electric field $g_1(t)$ decays from 1 to 0, and thus the amplitude *A* equals one. The parameter β characterizes the width of the distribution of relaxation times: for a narrow single mode distribution, $\beta = 1$, and the equation turns into a trivial single-exponential decay, whereas for a broad unimodal (or multimodal) distribution $\beta < 1$.

Ultracentrifugation. Ultracentrifugation was performed with an analytical ultracentrifuge MOM 3170B (Hungary) at 50 000 rpm at different temperatures from 4.5 to 23 °C. The concentration of pNIPA in the reference solution and in the solution of interpolymer complexes was 8 mg mL⁻¹.

Morphological Analysis. Visual observation of the morphology of the polymer mixtures was carried out during heating and cooling in a thermostat, the temperature of which was changed at a constant rate of about 1 °C min⁻¹. The photos were taken with a digital camera.

Results and Discussion

Poly(*N*-isopropylacrylamide) is a polymer with the lower critical solution temperature (LCST).³ The cloud point of its aqueous solution is ca. 33 °C. HS-DSC reveals a sharp asymmetric peak of heat capacity with $T_t = 33.5$ °C and $\Delta_t h = 55$ J g⁻¹ in the phase transition region (Figure 1). The phase separation results in a substantial decrease in the partial heat capacity of the polymer. The transition heat capacity increment is $\Delta_c p = -0.8$ J g⁻¹ K⁻¹. The negative value of the transition heat capacity increment points to a decreased accessible surface area of the hydrophobic groups of the polymer in the concentrated phase.³⁰ The small transition width $\Delta_t T = 0.8$ °C implies high cooperativity of the phase separation. The pNIPA phase behavior in the buffers used in the experiments was the same as in water.

The effects of poly(methacrylic acid) on the phase behavior of pNIPA and the thermal properties of the hydrogen-bonded pMAA/pNIPA interpolymer complexes were investigated. In the range of pH (pH 3–7) and polymer concentrations (0.01–10 mg mL⁻¹) studied in this work, pMAA shows no specific thermal properties.³¹ It means that no transitions related to pMAA itself could be expected for the pMAA/pNIPA mixtures in the calorimetric studies.

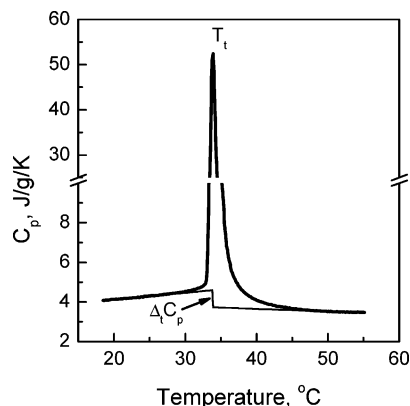


Figure 1. Apparent heat capacity curve of pNIPA in aqueous solution. Phase transition parameters derived from the curve are the temperature $T_t = 33.5$ °C, the enthalpy $\Delta_t h = 55$ J g⁻¹, the width $\Delta_t T = 0.8$ °C, and the heat capacity increment $\Delta_t c_p = -0.8$ J g⁻¹ K⁻¹. Polymer concentration is 2 mg mL⁻¹; heating rate is 1 °C min⁻¹.

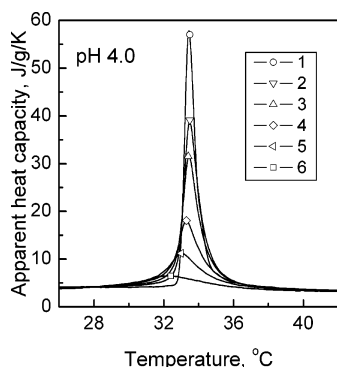


Figure 2. Apparent heat capacity curves for pNIPA (1) and for pMAA/pNIPA mixtures (2–6) at pH 4.0. pMAA/pNIPA ratio r : 0.27 (2), 0.67 (3), 1.3 (4), 2.0 (5), and 2.7 (6). Concentration of pNIPA is 1 mg mL⁻¹; 10 mM acetate buffer.

Figure 2 shows the heat capacity curves of the pNIPA solution and of the pMAA/pNIPA mixtures with different compositions at pH 4.0. With increasing the polymer molar ratio a pronounced change in the transition peak of pNIPA is observed: it decreases in height, increases in width, and slightly shifts toward lower temperatures. The transition profile becomes more symmetric. For mixtures with $r > 3$ no transitions were observed calorimetrically at pH 4.0.

Calorimetric results for pMAA/pNIPA mixtures of different compositions obtained at pH 4.0, 5.0, and 7.0 are summarized in Figure 3. Dependencies of the transition parameters (transition temperature, enthalpy, and width) on the molar polymer ratio are presented. The dashed lines indicate the pNIPA transition parameters. We can see that at pH 7.0 all the transition parameters for the polymer mixtures coincide with those obtained for pure pNIPA. This shows that no strong interaction takes place between pNIPA and pMAA at pH 7.0; i.e., polymers are mixed in the solution, and no interpolymer complexes are formed. These conditions correspond to the high ionization degree of pMAA, since it has $pK_{\text{int}} = 4.85$.³² Note that the presence of pMAA in the mixture even at high excess (ca. 100-fold) does not affect the pNIPA phase transition at pH 7.0, whereas at pH 4.0 and 5.0 coherent changes in the transition parameters for pMAA/pNIPA mixtures are observed. Thus, the transition temperature decreases slightly (3–4 °C) with increasing content of

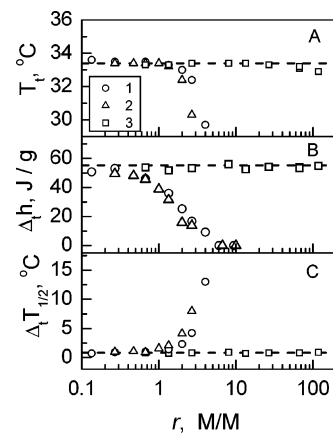


Figure 3. Transition temperature (A), enthalpy (B), and width (C) for pMAA/pNIPA mixtures vs the pMAA/pNIPA ratio r at pH 4.0 (1), 5.0 (2), and 7.0 (3). Dashed lines show the corresponding transition parameters for pNIPA.

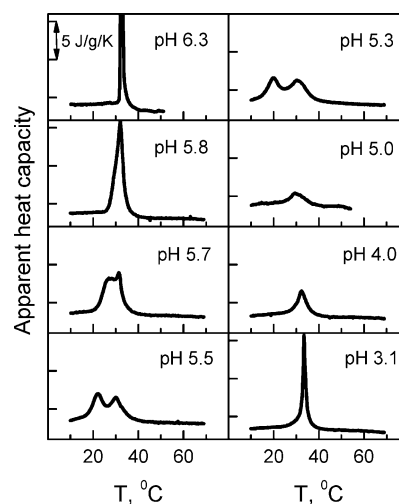


Figure 4. Apparent heat capacity curves of the pMAA/pNIPA mixture ($r = 2.7$) at different pH. The concentration of pNIPA is 1 mg mL⁻¹.

pMAA (Figure 3A). The transition enthalpy decreases dramatically, reaching zero (Figure 3B), while the transition width increases by more than 1 order of magnitude (Figure 3C). All the changes occur in a narrow range of r from 1 to 5, thus indicating the cooperative character of the complex formation. It is of interest that the mixtures with $r = 2.7$ were soluble at pH 5.0 but showed a slight opalescence at pH 4.0.

We performed a more detailed study of the phase transition in the mixtures within the pH range corresponding to the complex formation at constant mixture composition ($r = 2.7$). These results are shown in Figure 4. At pH 6.3 the transition peak of the mixture is similar to that of pNIPA. At pH 5.8 a noticeable decrease of the peak height is observed together with its broadening. At pH 5.7 the transition peak splits into two components: one at about 32 °C and another at lower temperature. At pH 5.5 and 5.3 two distinctive symmetric peaks are observed. The position of the higher temperature peak is close to that of pNIPA; the lower temperature peak is shifted toward lower temperatures. Both peaks are much wider than the peak of pure pNIPA. At pH 5.0 only one transition peak (obviously, the higher temperature peak) is observed, indicating the disappearance of the lower temperature transition. At pH 4.0 a single symmetric peak is observed. Its position

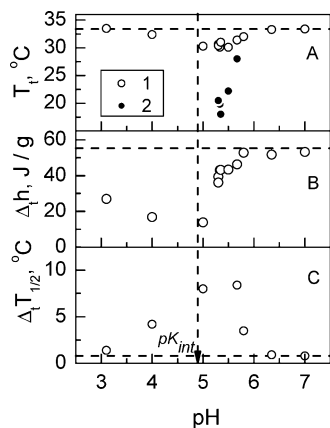


Figure 5. pH dependencies of the transition temperature (A), enthalpy (B), and width (C) of the pMAA/pNIPA mixture ($r = 2.7$): higher temperature peak (1) and lower temperature peak (2). The horizontal dashed lines show the corresponding transition parameters of pure pNIPA. The vertical dashed lines indicate pK_{int} of pMAA.

corresponds to that of pNIPA, but the peak width is significantly larger than that of pNIPA. Finally, at pH 3.1 a high narrow peak is seen that differs from the pNIPA peak by a more symmetric profile. Note that the solution at pH 4.0 was slightly opalescent and at pH 3.1 turned into a fine suspension.

The transition parameters of pMAA/pNIPA complexes vs pH at $r = 2.7$ are shown in Figure 5. As previously, horizontal dashed lines represent the transition parameters of the pNIPA solution. The vertical dashed line indicates pK_{int} of pMAA.³² The complexes obtained at pH to the right and to the left of this line were soluble and insoluble at room temperature, respectively, and had different transition parameters. For the soluble complexes two transition temperatures were observed (Figure 5A). The higher transition temperature decreases with decreasing pH very slightly (curve 1). The lower transition temperature decreases dramatically with decreasing pH and at pH < 5.3 falls below the lower temperature limit of the calorimeter (curve 2). The transition enthalpy of the soluble complexes decreases significantly with decreasing pH (Figure 5B). The transition width of soluble complexes notably increases with decreasing pH (Figure 5C). The results for the solutions with pH 5.5 and 5.3 are not shown in Figure 5C since the two peaks observed in this pH range are not well separated, and thus the transition width cannot be precisely estimated.

Dramatic changes of the transition parameters of soluble complexes take place within a narrow pH range from pH 5.8 to 5.0, indicating a strong pH sensitivity of the pMAA/pNIPA complexes. In the pH region, where the insoluble complexes are formed (pH $< pK_{\text{int}}$ of pMAA), they show properties similar to those of pNIPA as pH decreases. Thus, the transition temperature tends to that of pure pNIPA (Figure 5A). The transition enthalpy increases with decreasing pH remaining, however, below that of pure pNIPA (Figure 5B). The transition width decreases approaching the width of the pNIPA transition. However, the transition profile for the insoluble complexes is different from that of pNIPA: it is practically symmetrical.

Thus, the calorimetric data indicate significant transformations of the phase behavior of pNIPA upon complexing with pMAA. The nature of the interpolymer complexing is hydrogen bonding between the amide

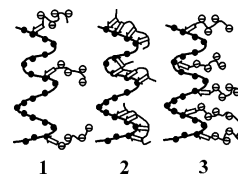


Figure 6. Schematic presentation of the structure of the pMAA/pNIPA complexes at different pH and pMAA/pNIPA molar ratio: pH $> pK_{\text{int}}$ of pMAA, low r (1); pH $< pK_{\text{int}}$ of pMAA, low r (2); and pH $> pK_{\text{int}}$ of pMAA, high r (3). Arrows and open and closed circles represent the protonated and the ionized carboxylic groups of pMAA and the amide groups of pNIPA, respectively.

groups of pNIPA and the protonated carboxylic groups of pMAA.^{18–21,33} Therefore, two main factors affect properties of the complexes: pH and content of pMAA in the complex. The number of hydrogen bonds formed by the pNIPA chain increases with decreasing pH and with increasing the pMAA content. In general, these two factors affect the pNIPA transition parameters in the same manner. They reduce slightly the transition temperature (Figures 3A and 5A), decrease strongly (to zero) the transition enthalpy (Figures 3B and 5B), and make the transition much broader (Figures 3C and 5C). The latter fact points directly to a reduced cooperativity of the pNIPA phase transition in the complexes. The cooperativity seems to be related to the length of the pNIPA blocks, which are not complexed with pMAA and thus participated in the transition. The greater is the length of these blocks, the higher is the cooperativity of the transition.³⁴ Consequently, the first conclusion following from the calorimetric data is that the enhanced interaction between pNIPA and pMAA results in shortening of the pNIPA hydrophobic blocks participating in the phase transition.

The effect of the mixture composition and pH on the structure of the pMAA/pNIPA complexes can be schematically represented in the following way (Figure 6). At high pH (pH $> pK_{\text{int}}$) the number of hydrogen bonds between pMAA and pNIPA is relatively small since carboxylic groups of pMAA are mainly ionized. If the pMAA content in mixture is low, pNIPA properties are affected only slightly, and the length of the hydrophobic pNIPA blocks in the complexes is long enough to provide high cooperativity of the phase transition (Figure 6, complex 1). At low pH (pH $< pK_{\text{int}}$) the number of hydrogen bonds that can be formed between pMAA and pNIPA increases due to the protonation of carboxylic groups of pMAA. In this case, a multipoint adsorption can take place, and the pNIPA chain is substantially modified even at low content of pMAA in the mixture (Figure 6, complex 2). In such a complex the pNIPA hydrophobic blocks are much shorter; this results in a low transition cooperativity. The complexes of this type tend to precipitate below LCST of pNIPA (insoluble complexes mentioned above). At high pH and high pMAA content, the pNIPA chains are substantially altered because of the high degree of binding of pMAA (Figure 6, complex 3). The ionized chains of pMAA make the complex strongly charged. Such a complex is soluble and characterized by lower enthalpy and lower cooperativity of the phase transition.

For all the types of the complexes shown in Figure 6, one could expect that hydrophilization of the pNIPA chain by conjugation with more hydrophilic pMAA should result in an increase in the LCST of pNIPA.^{4,13,35–37} Our data indicate quite the opposite

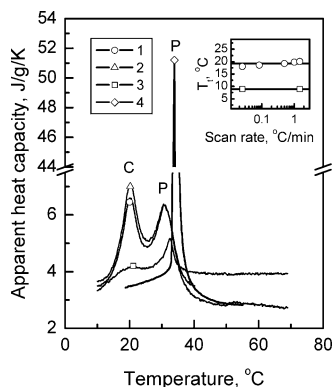


Figure 7. Apparent heat capacity curves for the pMAA/pNIPA mixture ($r = 2.7$) at pH 5.3: first scan to 40 °C (1), second scan to 70 °C (2), and third scan to 70 °C (3). Curve 4 shows the heat capacity curve of pure pNIPA. Peaks C and P correspond to the conformational transition and to the phase transition, respectively. The concentration of pNIPA is 1 mg mL⁻¹. Inset represents the temperature of the transition C of the pMAA/pNIPA mixture vs scanning rate in the heating (circles) and cooling (squares) mode.

(Figures 3A and 5A); i.e., the binding of a charged ligand (pMAA) leads to a decrease in the transition temperature. We can suggest so far no clear explanation of this paradox. It seems that the pNIPA chain loses its original features in the complexes with a high pMAA content, and the complex behaves as a new macromolecule with specific conformational properties. New conformational behavior of the complexes is illustrated by the multiple heat capacity transitions observed in the thermograms of the complexes under certain conditions (Figure 4). One of the possible explanations of the paradox can be the destruction of the hydrophobic hydration layer ("iceberg" melting) around the isopropyl groups of pNIPA as a result of the pMAA binding.

To shed more light on the nature of the cooperative transitions in the pMAA/pNIPA system, we performed a detailed study of the thermal behavior of the mixture with $r = 2.7$ at pH 5.3 using HS-DSC, ultracentrifugation, light scattering, and visual observation of the system.

The thermograms of the complex formed under these conditions are shown in Figure 7. The thermogram of pNIPA is presented in the same graph for comparison. Two heat capacity peaks C and P are observed for the complex at 20 and 30 °C (Figure 7, curve 2). The high-temperature peak P is located close to that of pNIPA but differs from it notably in terms of enthalpy and profile. Both C and P transitions are reversible after the heating of the solutions up to the temperature corresponding to the end of the peak P (40 °C) (Figure 7, curve 3). However, a clear irreversibility was observed after the heating of the mixture up to 70 °C (Figure 7, curve 4). This is surprising especially since the pNIPA phase transition is known to be completely reversible upon repetitive heating-cooling cycles in the range 10–100 °C and does not depend on the initial and final temperature. To investigate the thermodynamic nature of the transition C, we carried out calorimetric experiments at various heating rates in the heating and cooling mode. The result is presented in the inset to Figure 7. The transition temperature for the transition C of the complex does not significantly change with varying the heating rate from 0.03 to 1.5 °C min⁻¹. At the same time a hysteresis was observed. The transition C upon cooling was found at the temperature of about

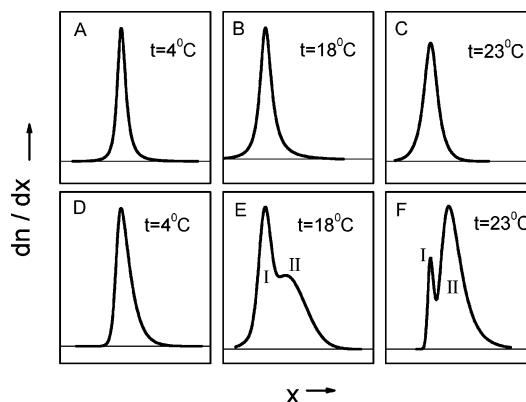


Figure 8. Sedimentation patterns of pNIPA (A–C) and of the pMAA/pNIPA mixture ($r = 2.7$) at pH 5.3 (D–F) vs temperature. The concentration of pNIPA in the reference and mixed solution is 8 mg mL⁻¹.

Table 1. Sedimentation Coefficients of pNIPA in the Reference Solution and of the Components of the pMAA/pNIPA Mixture ($r = 2.7$, pH 5.3) at Different Temperatures

t , °C	pNIPA	pMAA/pNIPA	
	$s_{20,w}$, S	$s_{20,w}^I$, S	$s_{20,w}^{II}$, S
4.5	1.0 ± 0.1	1.1 ± 0.1	
18	1.4 ± 0.1	1.5 ± 0.1	9.4 ± 0.6
23	1.6 ± 0.1	1.2 ± 0.2	17.5 ± 0.9

10 °C lower than that upon heating. Such a hysteresis is typically a sign of the disorder–order transitions in macromolecules.

Two main questions should now be answered: (i) What is the nature of the two cooperative transitions observed for the pMAA/pNIPA complex at 20 and 30 °C? (ii) What is the reason for the transition irreversibility after heating to 70 °C?

To elucidate the structural changes accompanying the transition C in the pMAA/pNIPA complexes, analytical ultracentrifugation at various temperatures was performed with a reference pNIPA solution and with the mixture ($r = 2.7$, pH 5.3). For the methodological reasons, the concentration of pNIPA in both systems was increased up to 8 mg mL⁻¹. To take into account the effect of the mixture concentration on the conformational transition of the complex, we performed calorimetric studies on the pMAA/pNIPA mixture at pNIPA concentration of 8 mg mL⁻¹. Two heat capacity peaks observed at the temperatures 18 and 31 °C were similar to those observed at lower concentration and thus indicated that the effect of polymer concentration is rather small. The end of the transition represented by the lower temperature peak corresponds to 23 °C; therefore, the sedimentation experiments were done at the temperatures 4.5, 18, and 23 °C. The sedimentation patterns are shown in Figure 8, and the sedimentation coefficients obtained are summarized in Table 1.

During the sedimentation pNIPA in the reference solution moves as an individual component at all temperatures studied (Figure 8A–C). The sedimentation coefficient of pNIPA increases from 1.0 S up to 1.6 S upon temperature increasing from 4.5 up to 23 °C (Table 1). The pMAA/pNIPA complex displays the sedimentation behavior at 4.5 °C similar to that of pure pNIPA (Figure 8D, Table 1), indicating that the hydrodynamic properties of the complex at low temperatures were determined mainly by the pNIPA component. At the temperature 18 °C (that corresponds to the maxi-

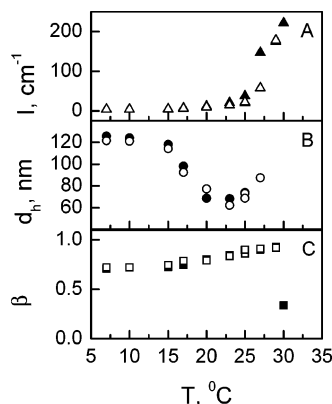


Figure 9. Temperature dependencies of the intensity of scattered light (A), the mean hydrodynamic diameter (B), and the distribution width parameter (C) for the pMAA/pNIPA mixture ($r = 2.7$) at pH 5.3. Concentration of pNIPA is 1 mg mL^{-1} . Closed and open symbols correspond to the slow and fast heating, respectively.

imum of the transition *C* of the complex) two components were seen in the sedimentogram (Figure 8E): the slow one (I) and the fast one (II) with the sedimentation coefficients of 1.5 and 9.4 S, respectively. At the temperature 23 $^{\circ}\text{C}$ (that corresponds to the end of the transition *C*) the fast component becomes dominating (Figure 8F), and its sedimentation coefficient increases up to 17.5 S.

We believe that two factors can cause a temperature-dependent increase in the sedimentation coefficient of a macromolecule: intramolecular chain collapse (folding) or association of chains (micellization). Certainly, these two processes can concur. We attempted to clarify this issue using light scattering.

Measurements of the scattered light intensity I , the mean hydrodynamic diameter d_h , and the distribution width parameter β were performed in the heating mode from 7 to 31 $^{\circ}\text{C}$. Two heating regimes were used: the slow one (ca. $0.02 \text{ }^{\circ}\text{C min}^{-1}$) and the fast one (ca. $1 \text{ }^{\circ}\text{C min}^{-1}$). The results are shown in Figure 9. The scattered light intensity was small at low temperatures and did not change up to 25 $^{\circ}\text{C}$ upon heating (Figure 9A). At temperatures above 25 $^{\circ}\text{C}$ the intensity increased considerably, indicating the phase separation of the system. However, the mean hydrodynamic diameter decreases markedly already above 15 $^{\circ}\text{C}$ (Figure 9B). This temperature corresponds to the onset of the transition *C* in Figure 7. At temperatures of ca. 23–25 $^{\circ}\text{C}$ that correspond to the end of the transition *C* the mean hydrodynamic diameter is about twice less than that at temperatures before the transition *C*. The parameter β increases slightly upon heating and reaches its maximum of 0.92 around 27 $^{\circ}\text{C}$. The value of this parameter close to 1.0 is characteristic of a narrow size distribution, which is typical of interpolymer complexes formed by oppositely charged polyelectrolytes.^{38,39}

Note that dynamic light scattering yields a monomodal size distribution contrary to the bimodal one detected by ultracentrifugation (Figure 8), though the same experimental conditions were used in both methods. At temperatures below 23–25 $^{\circ}\text{C}$, the solutions scattered light weakly and the distributions were broad. The width parameter β is of 0.7–0.8 and typical for broad size distributions. An origin of the apparent monomodality might be strong scattering from the larger particles, which screens partially or even totally scattering from the smaller particles, whereas the size

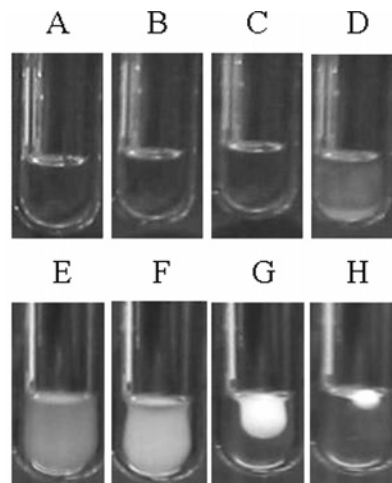


Figure 10. Morphology of the pMAA/pNIPA mixture ($r = 2.7$, pH 5.3) at different temperatures: 13 (A), 20 (B), 25 (C), 30 (D), 40 (E), 56 (F), 62 (G), and 70 $^{\circ}\text{C}$ (H). The pictures were taken during heating of the samples with the rate of ca. $1 \text{ }^{\circ}\text{C min}^{-1}$. The pNIPA concentration is 1 mg mL^{-1} .

resolution of velocity sedimentation is much higher than that of dynamic light scattering.

All the structural parameters measured by light scattering within the temperature range 7–25 $^{\circ}\text{C}$ did not depend on the heating rate. This result is compatible with the independence of the transition temperature on the heating rate obtained for the transition *C* by HS-DSC (Figure 7, inset). At temperatures above 25–27 $^{\circ}\text{C}$ we observed a sharp increase of the light scattering intensity accompanied by the increase in the mean hydrodynamic diameter and decrease in the parameter β (Figure 9). All these changes manifest the aggregation of particles in the course of phase separation of the system.

Thus, the cooperative transition observed for the pMAA/pNIPA mixture at temperatures 15–25 $^{\circ}\text{C}$ is associated with an increase in the sedimentation coefficient and a decrease in the mean hydrodynamic diameter of the complexes. At these temperatures no significant changes in the light scattering intensity or size distribution width were found. Consequently, we can conclude that at these temperatures the pMAA/pNIPA complexes undergo an intramolecular cooperative conformational transition into a more compact state. The transition is reversible and thermodynamically controlled. These features allow us to consider it as a transition of the “coil-to-globule” (C–G) type.

We examined visually the changes in the solutions of pMAA/pNIPA mixture ($r = 2.7$, pH 5.3) upon heating from 10 to 70 $^{\circ}\text{C}$ with the heating rate of about $1 \text{ }^{\circ}\text{C min}^{-1}$. The same heating rate was used in the calorimetric experiments. Figure 10 represents the photos of the mixture in a glass test tube taken at the temperatures corresponding to the specific points of the heat capacity curve (Figure 7, curve 2). The solution was transparent at temperatures 13, 20, and 25 $^{\circ}\text{C}$ (Figure 10A–C). At 30 $^{\circ}\text{C}$, i.e., at the temperature of the second peak on the thermogram of the complex (Figure 7, curve 2), the system was slightly turbid (Figure 10D). This indicates a microphase separation. No precipitation was observed. At higher temperatures the system morphology underwent further changes that were not typical of the pNIPA phase separation. Turbidity of the mixture increased only slightly at 40 $^{\circ}\text{C}$ (Figure 10E) without evident precipitation. At 56 $^{\circ}\text{C}$ segregation of the system

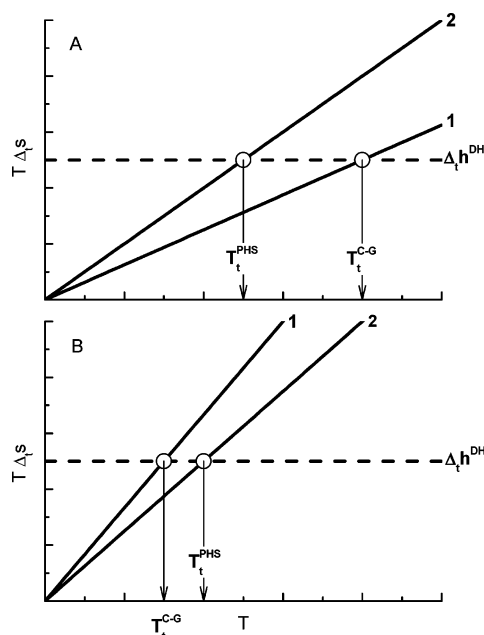


Figure 11. Schematic free energy diagrams for aqueous solutions of homopolymer (A) and heteropolymer (B): (1) entropic contribution to the transition free energy for the "coil-globule" transition, $T\Delta_{ts}^{C-G}$; (2) entropic contribution to the transition free energy for the phase separation transition, $T\Delta_{ts}^{PHS}$. The dashed lines show enthalpic contributions to the transition free energy that are represented mainly by the dehydration enthalpy, $\Delta_t h^{DH}$.

into two phases in the vicinity of the inner tube surface was observed (Figure 10F). At 62 °C a gel obviously appeared (Figure 10G) which became more shrunken at 70 °C (Figure 10H). The gel formation was reversible, and after slow cooling of the gel from 70 to 10 °C it disappeared. The gelation and the gel collapse were observed again upon second heating. However, if the cooling was performed quickly, the gel still existed at room temperatures. This behavior can explain the absence of reversibility of the thermogram of the pMAA/pNIPA complex after heating to 70 °C: the cooling in calorimetric cells was not slow enough and the gel "melting" was kinetically hindered. The formation of the thermotropic physical gel in the pMAA/pNIPA complexes was observed in the whole pH range 4.0 < pH < 6.3. This range of pH corresponds to the formation of the soluble pMAA/pNIPA complexes. The insoluble complexes did not form gels upon heating.

Finally, we would like to analyze in more detail the intramolecular "coil-to-globule" transition in the pMAA/pNIPA complex ($r = 2.7$, pH 5.3), which precedes phase separation, i.e., $T_t^{C-G} < T_t^{PHS}$ (Figure 7). Usually, homopolymers, like pNIPA, demonstrate the opposite behavior, $T_t^{C-G} > T_t^{PHS}$, at usual polymer concentrations.⁴⁰ Figure 11 represents schematic free energy diagrams for aqueous solutions of homo- and heteropolymer. For the "coil-globule" (C-G) and phase (PHS) transitions the entropic contributions are

$$T\Delta_{ts}^{C-G} = T(\Delta_{ts}^{DH} + \Delta_{ts}^{CONF})$$

$$T\Delta_{ts}^{PHS} = T(\Delta_{ts}^{DH} + \Delta_{ts}^{COMB})$$

where $\Delta_{ts}^{DH} > 0$ is the dehydration entropy; $\Delta_{ts}^{CONF} = (s_G - s_C) < 0$; s_G and s_C are entropies of the macromolecule in the globule and coil states, respectively; Δ_{ts}^{COMB}

< 0 is the change in the combinatorial entropy caused by the phase separation; $\Delta_t h^{DH}$ is the dehydration enthalpy being the main contribution to the transition enthalpy; T_t^{C-G} and T_t^{PHS} are transition temperatures for the coil-globule and phase separation transitions. For homopolymers, like pNIPA, $\Delta_{ts}^{CONF} < \Delta_{ts}^{COMB}$ at usual polymer concentrations, and consequently $T_t^{C-G} > T_t^{PHS}$, i.e., the phase separation precedes as a rule the coil-globule transition.⁴⁰ For heteropolymers, e.g. pNIPA/pMAA complexes, we can expect that the absolute value of the contribution Δ_{ts}^{CONF} becomes smaller, since the entropy of the macromolecule in the coil state, s_C , seems to decrease due to the microphase separation of the coil caused by the incompatibility of NIPA and MAA residues. This should lead to a decrease in the coil-globule transition temperature. At the same time, the combinatorial contribution Δ_{ts}^{COMB} would not change considerably in the case of heteropolymers. The reason is that Δ_{ts}^{COMB} is mainly determined by the translation degrees of freedom of macromolecules and depends on their internal degrees of freedom rather slightly. Thus, we can speculate that for the heteropolymers the coil-globule transition temperature, T_t^{C-G} , can be lower than the phase separation temperature, T_t^{PHS} , under appropriate conditions. Accordingly, heating can first induce the coil-globule transition and then the phase separation of the solution of globules. In addition, it is reasonable to note that the phase separation temperature of such a solution must be lower than that of the solution of coils of similar molecular weight. In fact, formation of internal virtual bonds between segments typical of the globule conformation implies an additional decrease in the solvent quality of water.⁴¹ Summarizing, we can conclude that the microphase separation of the pNIPA/pMAA complexes reduces their conformational entropy in the coil state and thus makes the coil-globule transition more favorable in comparison with the phase separation within a certain temperature range. After this transition we have a solution of globules instead of a solution of coils as in the case of pNIPA below the phase separation temperature. Since the solution of globules is osmotically less stable than the solution of coils,⁴¹ its phase separation temperature is lower than that of the solution of coils.

Conclusions

The phase transition of pNIPA is dramatically modified by complexing with pMAA. The pMAA/pNIPA complexes are characterized by a strong pH sensitivity of their phase and conformational behavior. Factors determining the complex composition (pH and polymer ratio) control the hydrophobic-hydrophilic balance in the complexes. Because of this balance, the complexes are able to undergo an intramolecular cooperative conformational transition from a coil state to a more compact folded state without loss of solubility.

Acknowledgment. The work was supported by the INTAS (Project 01-607). T.V.B., N.V.G., and V.Y.G. acknowledge financial support from Russian Foundation for Basic Research (Project 04-03-32355). The authors thank Mr. Alexander L. Leontiev for carrying out the velocity sedimentation experiments.

References and Notes

- (1) Khokhlov, A. R.; Khalatur, P. G. *Physica A* **1998**, 249, 253–261.

- (2) Wahlund, P. O.; Galaev, I. Y.; Kazakov, S. A.; Lozinsky, V. I.; Mattiasson, B. *Macromol. Biosci.* **2002**, *2*, 33–42.
- (3) Schild, H. G. *Prog. Polym. Sci.* **1992**, *17*, 163–249.
- (4) Hahn, M.; Gornitz, E.; Dautzenberg, H. *Macromolecules* **1998**, *31*, 5616–5623.
- (5) Berlinova, I. V.; Dimitrov, I. V.; Vladimirov, N. G.; Samichkov, V.; Ivanov, Y. *Polymer* **2001**, *42*, 5963–5971.
- (6) Konak, C.; Reschel, T.; Oupicky, D.; Ulbrich, K. *Langmuir* **2002**, *18*, 8217–8222.
- (7) Virtanen, J.; Holappa, S.; Lemmetyinen, H.; Tenhu, H. *Macromolecules* **2002**, *35*, 4763–4769.
- (8) David, G.; Alupe, V.; Simionescu, B. C.; Dincer, S.; Piskin, E. *Eur. Polym. J.* **2003**, *39*, 1209–1213.
- (9) Guo, R. W.; Lu, X. D.; Fang, D. B. *Chem. J. Chin. Univ.* **2003**, *24*, 1311–1314.
- (10) Lozinsky, V. I.; Simenel, I. A.; Kulakova, V. K.; Kurskaya, E. A.; Babushkina, T. A.; Klimova, T. P.; Burova, T. V.; Dubovik, A. S.; Grinberg, V. Y.; Galaev, I. Y.; et al. *Macromolecules* **2003**, *36*, 7308–7323.
- (11) Okhapkin, I. M.; Nasimova, I. R.; Makhaeva, E. E.; Khokhlov, A. R. *Macromolecules* **2003**, *36*, 8130–8138.
- (12) Dubovik, A. S.; Grinberg, V. Y.; Makhaeva, E. E.; Khokhlov, A. R. In *Actual problems of polymer chemistry: high-performance and ecologically safe processes of synthesis of natural and synthetic polymers and related materials*, 20–27 Aug 2002, Ulan-Ude, Scientific Centrum of Buryatiya of the RAS, p 51.
- (13) Chen, G. H.; Hoffman, A. S. *Nature (London)* **1995**, *373*, 49–52.
- (14) Meewes, M.; Ricka, J.; Desilva, M.; Nyffenegger, R.; Binkert, T. *Macromolecules* **1991**, *24*, 5811–5816.
- (15) Lozinsky, V. I.; Kalinina, E. V.; Putilina, O. I.; Kulakova, V. K.; Kurskaya, E. A.; Dubovik, A. S.; Grinberg, V. Ya. *Vysokomolek. Soed. A* **2002**, *44*, 1906–1914.
- (16) Siu, M.; Zhang, G. Z.; Wu, C. *Macromolecules* **2002**, *35*, 2723–2727.
- (17) Staikos, G.; Bokias, G.; Karayanni, K. *Polym. Int.* **1996**, *41*, 345–350.
- (18) Garay, M. T.; Llamas, M. C.; Iglesias, E. *Polymer* **1997**, *38*, 5091–5096.
- (19) Koussathana, M.; Lianos, P.; Staikos, G. *Macromolecules* **1997**, *30*, 7798–7802.
- (20) Staikos, G.; Karayanni, K.; Mylonas, Y. *Macromol. Chem. Phys.* **1997**, *198*, 2905–2915.
- (21) Garay, M. T.; Alava, C.; Rodriguez, M. *Polymer* **2000**, *41*, 5799–5807.
- (22) Liu, S. Y.; Jiang, M.; Liang, H. J.; Wu, C. *Polymer* **2000**, *41*, 8697–8702.
- (23) Yuan, X. F.; Jiang, M.; Zhao, H. Y.; Wang, M.; Zhao, Y.; Wu, C. *Langmuir* **2001**, *17*, 6122–6126.
- (24) Wang, L. Q.; Tu, K. H.; Li, Y. P.; Fu, J.; Yu, F. S. *J. Mater. Sci., Lett.* **2002**, *21*, 1453–1455.
- (25) Jiang, M.; Duan, H. W.; Chen, D. Y. *Macromol. Symp.* **2003**, *195*, 165–170.
- (26) Wang, L. Q.; Tu, K. H.; Li, Y. P.; Mang, J. *Chin. Chem. Lett.* **2003**, *14*, 407–410.
- (27) Nuopponen, M.; Ojala, J.; Tenhu, H. *Polymer* **2004**, *45*, 3643–3650.
- (28) Lim, K. T.; Webber, S. E.; Johnston, K. P. *Macromolecules* **1999**, *32*, 2811–2815.
- (29) Chu, B. *Laser Light Scattering: Basic Principles and Practice*; Academic Press: San Diego, 1991; p 74.
- (30) Grinberg, V. Y.; Dubovik, A. S.; Kuznetsov, D. V.; Grinberg, N. V.; Grosberg, A. Y.; Tanaka, T. *Macromolecules* **2000**, *33*, 8685–8692.
- (31) Nemec, J. W.; Bauer, W., Jr. In *Encyclopedia of Polymer Science and Engineering*; Mark, H. F., Bicales, N. M., Overberger, C. C., Eds.; John Wiley & Sons: New York, 1985; p 225.
- (32) Tanford, C. *Physical Chemistry of Macromolecules*; John Wiley & Sons: New York, 1961; p 550.
- (33) Bokias, G.; Staikos, G.; Iliopoulos, I. *Polymer* **2000**, *41*, 7399–7405.
- (34) Schild, H. G.; Tirrell, D. A. *J. Phys. Chem.* **1990**, *94*, 4352–4356.
- (35) Maeda, Y.; Yamamoto, H.; Ikeda, I. *Langmuir* **2001**, *17*, 6855–6859.
- (36) Qiu, X.; Kwan, C. M. S.; Wu, C. *Macromolecules* **1997**, *30*, 6090–6094.
- (37) Shibayama, M.; Tanaka, T. *J. Chem. Phys.* **1995**, *102*, 9392–9400.
- (38) Buchhammer, H. M.; Mende, M.; Oelmann, M. *Colloids Surf. A* **2003**, *218*, 151–159.
- (39) Holappa, S.; Andersson, T.; Kantonen, L.; Plattner, P.; Tenhu, H. *Polymer* **2003**, *44*, 7907–7916.
- (40) Grosberg, A. Yu.; Kuznetsov, D. V. *Macromolecules* **1992**, *25*, 1970–2003.
- (41) Kurata, M. *Ann. N.Y. Acad. Sci.* **1961**, *89*, 635.

MA0486851